Theoretical study of the mechanism of dry oxidation of 4*H*-SiC

Jan M. Knaup,* Peter Deák,† and Thomas Frauenheim
Department of Theoretical Physics, Faculty of Science, University of Paderborn, D-33095 Paderborn, Germany

Adam Gali
Department of Atomic Physics, Budapest University of Technology and Economics, Budafoki út 8, H-1111, Budapest, Hungary

Zoltán Hajnal
MTA Research Institute for Technical Physics and Materials Science, P.O. Box 49, H-1525 Budapest, Hungary

W. J. Choyke
Department of Physics and Astronomy, University of Pittsburgh, Pittsburgh, Pennsylvania 15260, USA
(Received 16 November 2004; revised manuscript received 24 January 2005; published 23 June 2005)

Possible defect structures, arising from the interaction of O_2 molecules with an ideal portion of the SiC/SiO_2 interface, have been investigated systematically using density functional theory. Based on the calculated total energies and assuming thermal quasiequilibrium during oxidation, the most likely routes leading to complete oxidation have been determined. The defect structures produced along these routes will remain at the interface in significant concentration when stopping the oxidation process. The results obtained for their properties are well supported by experimental findings about the SiC/SiO_2 interface. It is found that carbon-carbon bonds can explain most of the observed interface states but not the high density near the conduction band of 4*H*-SiC.

DOI: 10.1103/PhysRevB.71.235321 PACS number(s): 68.35.Ct, 73.20.Hb, 73.20.At

I. INTRODUCTION

The strong bonds in SiC result in high stability, good heat conductivity and a wide band gap (high breakdown field). This makes SiC very desirable for high power semiconductor applications. Additionally, SiC has SiO_2 as its native oxide, a unique advantage among the wide-gap semiconductors. This great advantage for device manufacturing is, however, still marred by the large density of interface states (D_{it}) at the SiC/SiO_2 interface, which has so far prevented the successful fabrication of metal-oxide-semiconductor (MOS) devices that meet application demands. [D_{it} gives the energy distribution of states in the gap, i.e., $D_{it}(E)$ is the surface density of states between E and $E+dE$.] As opposed to the Si/SiO_2 interface, where the D_{it} is nowadays less than $10^{10}\ \mathrm{cm^{-2}\,eV^{-1}}$, at the SiC/SiO_2 interface the D_{it} is $\sim 10^{11}\ \mathrm{cm^{-2}\,eV^{-1}}$ in the middle of the band gap and $\sim 10^{13}\ \mathrm{cm^{-2}\,eV^{-1}}$ or more at the band edges in 4*H*-SiC (the technically relevant polytype with the widest band gap). As a consequence, the channel mobility in MOS transistors is much lower than the bulk mobility, and insufficient for 4*H*-SiC high-power switches.

The measurement of $D_{it}(E)$ over the whole band gap is not possible using a single experimental technique. A collection of data on MOS structures with *n*- and *p*-type channels, can be found in Ref. 1 for 3*C*, 6*H*, and 4*H* polytypes, based on admittance spectroscopy (AS) and deep level transient spectroscopy (DLTS). The curve for 4*H*-SiC is schematically reproduced in Fig. 1. It shows a continuous distribution of states rising towards the band edges with various structures ($D_1 \approx E_V+0.3$ eV, $D_2 \approx E_V+0.8$ eV, $D_3 \approx E_V+1.8$ eV, and $D_4 \approx E_V+2.7$ eV) superimposed. The sensitivity of both methods is dependent on the energy relative to the band edges but the dependences are different. Therefore, the position of these structures (or even the existence of peaks) should be regarded with caution. Still, D_2 and D_4 in the D_{it} from DLTS in Ref. 1 can also be observed in the D_{it} obtained from capacitance-voltage (CV) measurements,[2] at about the same energy. X-ray photoelectron spectroscopy (XPS) studies on MOS structures under bias revealed a peak of states coinciding with D_3 in 6*H*-SiC.[3] The high density of interface states near the conduction band was found to be connected to traps with slower response times.[4] These states were also investigated[5] by photon stimulated tunneling (PST), locating a peak at $E_C-0.1$ eV. A peak in this range was also found[6] by CV and by TSC (thermally stimulated current) measurements.[7,8] In the latter study, a second set of slow states were also found, with an energy coincident with D_4. The nature of the individual parts of the D_{it} is also not established. The high density of states near the conduction band appear to be electron traps (acceptorlike) while the rest of the states appear to be hole traps (donorlike).

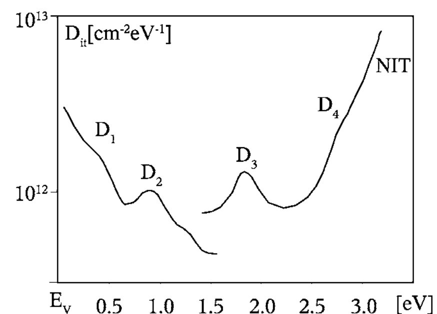

FIG. 1. Schematic overview of the experimental data about the D_{it} at the 4*H*-SiC/SiO_2 interface, after Ref. 1. For explanation, see the text.

 ©2005 The American Physical Society

It is generally assumed, that the oxidation process generates SiO_2 and emits CO, and that the latter can react to form graphitic carbon clusters at or close to the interface. It has been proposed,[9,10] that such carbon clusters at the interface cause the fast portion of the D_{it}, while the slow portion is assumed to originate from intrinsic defects, so-called near interface traps (NITs), in the oxide layer.

Unlike the Si/SiO_2 system, the interface between silicon carbide and its oxide is not chemically abrupt. It is easy to understand, that the removal of carbon, by whatever process, will not be immediately complete. X-ray photoelectron spectroscopy measurements show the presence of a $Si_4C_{4-x}O_2;x\leqslant 2$ transition layer of several nm in thickness.[11–13] The nature of this transition layer, i.e., its actual atomistic structure, is not yet well understood, but an enhanced carbon concentration could clearly be established.[3,14] Many authors suggest the presence of graphitic or sp^2-bonded carbon islands at the interface.[1,15,16] The observation of "platelet-shaped inhomogeneities" with lateral dimensions of 30–80 nm and thicknesses of 3–4 nm by atomic force microscopy (AFM) on the SiC side of the interface after etching off the oxide layer,[16] and the detection of increased carbon concentrations at the interface in areas of similar size by electron energy loss spectroscopy (EELS)[17] have been presented as the main evidence for the presence of such islands.

Comparisons of results obtained at SiC/SiO_2 interfaces and *a*-C:H films deposited on SiO_2,[1] led to the conclusion, that the bands of π-bonded carbon clusters are responsible for the continuously rising "background" states in the D_{it} , while discrete structures are caused by C-C σ-bonds. Earlier XPS observations of "═C═C═ units bonded to ═Si-O-Si═ of siloxene type bonds"[11] have been cited to support this suggestion. XPS measurements on MOS structures under bias[3] in 6*H*-SiC (Ref. 56) could directly correlate this part of the C1*s* spectrum to a peak at $E_V+1.8$ eV, coinciding with D_3.

The existence of Si-O-C bonds and "A-center-like defects" (i.e., carbon replaced by oxygen in the cage of four silicon atoms) could be inferred from XPS measurements[12] and positron annihilation spectroscopy (PAS)[18] experiments, respectively. Graphite at the interface could not yet be observed by XPS.[11,13] (Note though, that the sensitivity limit of XPS is 0.1 monolayers. If every carbon atom from an alleged graphitic carbon island would contribute one state to the D_{it}, a graphite concentration of ~0.01 monolayers would suffice to generate a D_{it} of 10^{13} cm^{-2} eV^{-1}.)

Very recently, in surface enhanced Raman (SER) measurements,[19] a carbon related peak was observed on the C face of oxidized SiC, after etching of the oxide and sputter-deposition of a metal (Ag or Au) layer. After deconvolution, this peak has been assigned to stretching mode vibrations of a primarily two-dimensional *ideal* graphite (*G* peak) with some contribution from *disordered or defective* graphite (*D* peak), and polyenes. The size of the structures was estimated to be $\leqslant$2 nm. A similar, broad "*G* peak" was also found on the Si face, with an intensity less by almost an order of magnitude, but no *D* peak. Considering the higher D_{it} on the *C* face with respect to the Si face prior to postoxidation anneals, the authors suggest these graphitic "flakes," giving rise to the "*G* peak," to be the cause of the difference. It should be noted that, considering the vanishing "*D* peak" (defective or disordered graphite) for a carbon aggregation with graphitic feature sizes below 2 nm, makes the assignment of the "*G* peak" to ideal graphite planes problematic, because in such cases the *D* peak should be even higher than the *G* peak.[20]

The fact, that hydrogen annealing does not substantially lower the D_{it} is strong evidence, that the interface states do not primarily originate from silicon dangling bonds.[9,10] The presence of C dangling bonds, however, has been proven by electron paramagnetic resonance (EPR).[21,22]

Theoretical modeling of the interface between crystalline SiC and vitreous SiO_2 is very difficult. Defects of the interface have so far only been considered either in the SiC (Ref. 23) or in the SiO_2 phase.[15] Therefore, the origin of the D_{it} at the 4*H*-SiC/SiO_2 interface is so far not well understood and only limited information about the atomistic structure of the interface exists.

Nitridation techniques (either oxidation in NO or postoxidation thermal annealing in N_2O) have been used with considerable success for some time now, to improve the interface quality.[2,7,8,24–27] However, the reasons for these improvements have not yet been well understood either, and are subject to controversial discussions in the literature. This is partly due to the fact that the mechanism of the dry oxidation of SiC is still unclear. Understanding the dry oxidation process is a vital step towards an understanding of the processes, which lead to the improvements of the D_{it} achieved by nitridation.

In this work, we will examine the chemical reactions which could take place during the dry oxidation of 4*H*-SiC, in order to identify the dominant interface defects generated during this process. We will relate the calculated properties of the dominant interface defects to the available experimental data in order to gain information about the atomistic structure of the interface, and the origin of the different D_{it} features. Preliminary results on the oxidation route, leading to stochiometrically perfect oxide, have been presented at the ICDS-22 conference.[28] Some of those data have been corrected and the investigations were extended to carbon incorporation at the interface via multiple carbon defects.

II. METHODS

A. Modeling the reactions

The initial oxidation of the clean SiC surface is not investigated here, it is rather assumed, that an oxide layer has already formed. The basis for modeling the reaction sequences of the dry oxidation process is a model of a defect-free portion of the SiC/SiO_2 interface. We employ a two-dimensional (2D) periodic supercell ("slab"), containing four (0001) double-layers of 4*H*-SiC and two SiO_2 layers, fitted to the Si terminated surface of the SiC part in such a way that the SiC surface is terminated without defects or dangling bonds (cf. Fig. 2). The dangling bonds on the C-terminated surface are saturated with H atoms, while those on the SiO_2 surface with O and H atoms. The 2D supercell consists of 4×4 surface primitive cells, i.e., 128 atoms in the SiC and

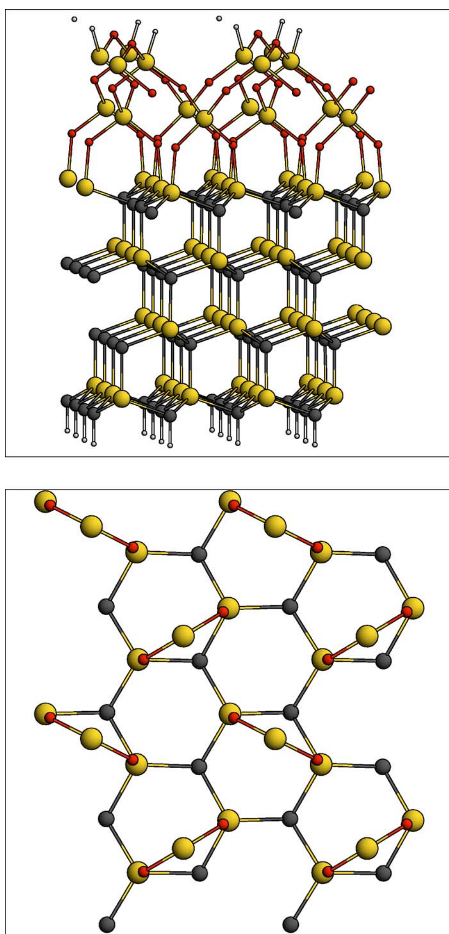

FIG. 2. (Color online) The interface model [O, small, dark grey (red) spheres; C, medium sized black spheres; Si, large, light grey (yellow) spheres, H, small light grey spheres].

48 atoms in the SiO_2 parts, as well as 28 terminators, altogether 204 atoms. Considering the size of the cell, the Γ-point approximation is used. (The calculated band gap agrees well with that obtained for bulk 4*H*-SiC.)

Based on this model, possible interactions between the initially defect-free interface and sequentially arriving O_2 molecules are considered. (Recent theoretical work[29] has proved that, in accordance with the Deal-Grove model, the dominating diffusion species in the oxide during dry oxidation is the O_2 molecule.) Following Ref. 15, only the energies of stable states will be calculated. Since the oxidation of SiC is a very slow process even at the usually applied high temperature of $\sim 1200\ ^\circ\mathrm{C}$, thermal quasiequilibrium can be assumed. From this follows that the relative occurrence of alternative reactions will be determined by the reaction energies. The predominant interface defects can be identified by finding the most likely reaction paths leading to the oxidation of the silicon carbide. Obviously, this approach is not sufficient to establish the kinetics of the oxidation. Also, our modeling efforts do not account for global stress-induced effects. In general, our approach is aimed only at establishing the main routes of oxidation and the characteristic interface defects. A large number of defect configurations, which could arise from the simultaneous interaction of two oxygen atoms with the interface, was investigated, also allowing for C or CO removal by out diffusion through the oxide. For the energies of the CO and O_2 molecules, the energies of the free molecules were chosen, since they can diffuse fast through SiO_2.[30,31]

In addition to the interface model described above, a 243-atom $3\times3\times3$ supercell of α-quartz (in the Γ-point approximation) was used to model defects in the oxide layer, further away from the interface, for the purpose of calculating the energies of reactions leading to C or Si emission into the oxide or for correction purposes (cf. Sec. II B). Also for correction purposes, a 64-atom SiC supercell (with a 2^3 MP *k*-point set[32]) was applied.

The reaction energies are calculated by summing the total energies of the reaction products and subtracting the total energies of the educts.

B. Calculation procedure

SiC (as well as SiO_2) is a wide band gap material, therefore the typical gap error in standard implementations of density functional theory—which also influences the relative energies of defects through incorrect level positions in the gap—can be significant. In order to avoid the consequences in comparing different reactions, the total energy must be corrected. Because of the large models employed in this work, an efficient scheme for calculations is necessary to save computer time. Therefore, a three-step procedure for geometry optimization and electronic structure calculation was employed.

In the first step, the initial geometries were optimized using the very efficient self-consistent charge, density functional based, tight-binding (SCC-DFTB) method[33] as implemented in the DYLAX package. A set of Slater-Koster files, tested for the Si-O-C system,[30] was employed. The geometry optimizations were performed using a conjugate gradient (CG) algorithm, until the interatomic forces fell below 10^{-4} a.u.(~ 0.016 eV/Å). In our experience, this method produces final geometries that are in accord with full DFT calculations. Additionally, this method does reproduce the energetic order of different metastable configurations of similar defects quite well. Because of this and the high speed of the DFTB method it is possible, to test many different competing configurations and select the most stable variants for further investigation.

In the second step, the DFTB output geometry was refined by CG relaxation based on *first-principles* density functional theory (DFT) calculations in the local density approximation (LDA) using the SIESTA (Ref. 34) code. These calculations were performed using a matrix diagonalization solver for the Kohn-Sham equations (i.e., not the order-*N* option of SIESTA). For this work, pseudopotentials in the Troullier-Martins formulation[35] with core radii of $r_C=1.14, r_O=1.25$ and $r_{Si}=1.89$ Bohr were selected. Numerical atomic orbitals corresponding to a "double-ζ" valence basis with polarization functions were used. The Ceperley-Alder[36] exchange-correlation functional in the Perdew-Zunger parametrization[37] was employed. Experience shows, that the number of CG steps required to reach the relaxed geometry

can be reduced considerably by the DFTB prerelaxation. The relaxation was performed until the interatomic forces were below 0.016 eV/Å. Test calculations on defects in bulk SiC (Ref. 38) and Si (Ref. 39) have shown, that the SIESTA final geometries obtained with these parameters are in good agreement with well-converged plane-wave LDA calculations.

In the last step, approximate corrections for the LDA gap error were made. The interface defects considered here can be classified according to their nearest-neighbor environments as "SiC" or "SiO_2-defects." In each case, an analogous defect was placed into a bulk SiC or SiO_2 supercell. An LDA and a hybrid functional[40,41] calculation was then carried out for the bulk defect. (The geometry obtained by LDA was held fixed during the hybrid functional calculation.) The total energy of the LDA calculation at the interface was then corrected by the difference in the positions of occupied defect levels relative to the VB edge, between the hybrid functional and the LDA values in the bulk. The corrected total energies were then used to calculate the reaction energies. (All energy values cited in this paper are corrected.)

It has been shown that hybrid functionals can reproduce the band gaps of solids consistently well.[42,43] Following the suggestion of Becke,[44] a one-parameter hybrid functional was used in this work.

For the hybrid functional calculations in bulk SiC and α-quartz, the CRYSTAL (Ref. 45) code was used with norm-conserving Durand-Barthelat[46] pseudopotentials and a $21G^*$ valence basis[47] optimized for these pseudopotentials. Like in SIESTA, the Ceperley-Alder exchange-correlation functional in the Perdew-Zunger parametrization was used, with the exchange part mixed with exact exchange following the equation

$$E_{\mathrm{XC}} = E_{\mathrm{XC}}^{\mathrm{LSDA}} + \lambda(E_{\mathrm{X}}^{\mathrm{exact}} - E_{\mathrm{X}}^{\mathrm{LSDA}}). \quad (1)$$

For α-quartz we have used $\lambda = 0.28$, as suggested by Becke.[44] Earlier work on SiC has shown that the value $\lambda = 0.20$ reproduces the band gap of different polytypes very well,[38] so in the case of SiC this value was used.[57,55]

III. IMPORTANT INTERFACE DEFECTS

We have studied the possible reactions of an O_2 molecule with the interface in a systematic way, investigating: (i) reactions without the emission of host atoms, (ii) reactions in which an emitted host C atom leaves the interface in form of a CO molecule, and (iii) reactions with C or Si emission, considering both incorporation of these at the interface and their emission into the oxide. Then we have also considered interaction and complex formation of C atoms incorporated at the interface.

In each case, we have calculated many different configurations of the possible resulting defects, guided by chemical intuition and experience with defects in semiconductors.[58]

Most of the defects we have found here, are known from the bulk material. We have, however, also come across several defect configurations that are specific to the interface. Here we describe the most important of these.

Interstitial oxygen at the interface—O_i^{if}: In contrast to the situation in bulk SiC, where oxygen has been shown to prefer the carbon substitutional site,[48] at the SiC/SiO_2 interface an interstitial configuration, where the oxygen buckles out of the SiC side into the oxide phase [Fig. 3(a)], is preferred. The O_i^{if} is essentially a C-O-Si bridge and it is electrically inactive.

Carbon vacancy at the interface, saturated by two oxygen atoms—V_CO_2 : The carbon vacancy at the interface can accommodate two oxygen atoms [Fig. 3(b)], but only one of them is sitting in the cage of the four Si neighbors, binding to two of them. The other oxygen buckles out toward the oxide phase. Therefore, from the viewpoint of positron annihilation spectroscopy (PAS), it resembles the *A* center (VO defect) in silicon.[49,50] This defect is also electrically inactive.

It should be pointed out, that the V_CO_2 complex is stochiometrically equivalent to one SiO_2 unit. However, the specific volume of Si in V_CO_2 is the same as in SiC, which is only about half the value in SiO_2. Therefore, extensive structural rearrangement of the newly formed oxide must take place. It is outside the scope of this work, to consider these processes, which finally lead to the vitreous structure of the oxide layer.

Carbon interstitial sharing a lattice carbon site at the interface–$(C\text{-}C_i)_C$: (At the interface, the two C atoms of the split pair are no longer equivalent. The notation has been chosen to make equations of reaction easier to follow.) The carbon split interstitial, shown in Fig. 3(c), is composed of two sp^2 hybridized carbon atoms. However, the planes of their sp^2 orbitals are nearly perpendicular, which results in a single σ bond between them. From this follows that two, originally half-filled, *p* orbitals remain. The nearby interface causes these to be no longer equivalent, so that one *p* orbital is filled, while the other is empty. (However, this singlet state is only 0.25 eV lower in energy than a triplet one, with both *p* orbitals half-filled.)

$(C\text{-}C_i)_C$ is electrically active, the levels of the *p* states are at $E_V + 1.4$ eV and $E_V + 1.9$ eV. We have found that $(C\text{-}C_i)_C$ defects are created simultaneously with V_CO_2, as interstitial carbon is ejected upon capture of an O_2 molecule. The complex, $V_CO_2 + (C\text{-}C_i)_C$, as shown in Fig. 3(d), is energetically favorable. In this complex the gap levels are shifted to $E_V + 1.0$ eV and $E_V + 1.8$ eV, respectively.

Pair of carbon interstitials—$(C_i)_2$ (Fig. 4): Two interstitial carbon atoms may form a doubly bonded dimer (with C atoms in puckered bond-center position). This is a very stable and inert defect, having an occupied gap state at $E_V + 0.43$ eV but no unoccupied state in the 4*H*-SiC band gap. The occupied state shifts between $E_V + 0.37$ eV and $E_V + 0.51$ eV, depending on the number $n = 0,1,2$, of nearby V_CO_2 units.

IV. THE DRY OXIDATION PROCESS

The dry oxidation process of SiC was modeled by investigating the possible reactions of O_2 molecules arriving sequentially at the interface. The calculated reaction energies for the possible oxidation sequences are shown in Fig. 5. As can be seen, from the many possibilities, two reaction paths emerge as energetically dominant. These (marked by thick lines—in color red and green—in Fig. 5) will determine

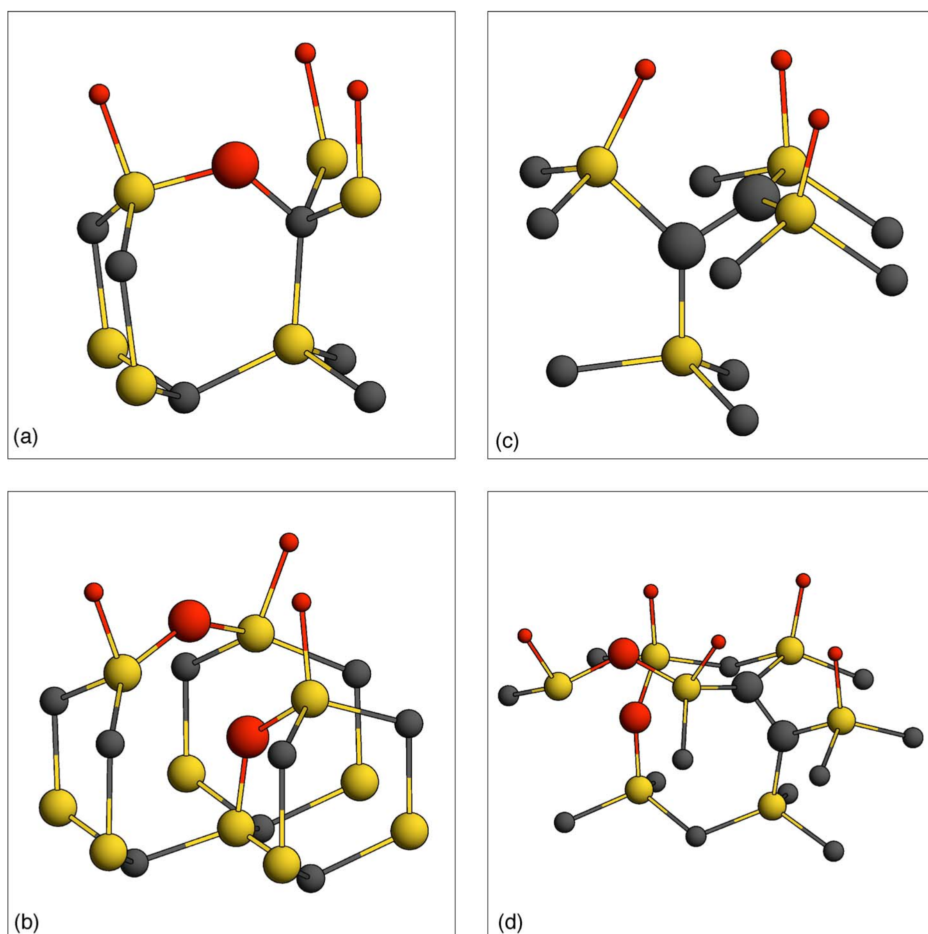

FIG. 3. (Color online) The most important interface defects, viewed nearly parallel to the interface, SiO_2 on top. [O, small, dark grey spheres (red) C, medium sized black spheres; Si, large, light grey spheres (yellow) defect atoms are marked by large spheres.]

which defects will be most abundant during the dry oxidation of SiC.

The simplest interaction between the defect-free SiC/SiO_2 interface and an arriving O_2 molecule is the incorporation of both oxygens in the form of two neighboring interstitials,

$$\mathrm{SiC/SiO_2^{perf}} + \mathrm{O_2^g} \rightarrow 2(\mathrm{O}_i^{if}). \quad (2)$$

We have found that this reaction is exothermic, yielding 2.0 eV. Of course, this process could be repeated for consecutive O_2 molecules, but this would not lead to an oxidation of SiC, only to the saturation of the interface with interstitial oxygen. (Interstitial oxygen is unstable in the bulk.) Actually, continuing O_i incorporation will be hindered by the increasing stress at the interface.

Figure 5 shows that it is slightly more favorable to form a V_CO_2 unit, by ejecting a C atom into an interstitial position, thus forming a V_CO_2+$(C\text{-}C_i)_C$ complex,

$$\mathrm{SiC/SiO_2^{perf}} + \mathrm{O_2^g} \rightarrow \mathrm{V_CO_2} + (\mathrm{C\text{-}C}_i)_\mathrm{C}. \quad (3)$$

All other possible reactions examined are significantly less favorable.

Upon arrival of a second O_2 molecule, the energetically most favorable configuration, starting either from $2(O_i^{if})$ or from V_CO_2+$(C\text{-}C_i)_C$ is an O_i^{if}+V_CO_2 complex. In both cases the reaction is accompanied by CO emission. In the former the reaction is

$$2(\mathrm{O}_i^{if}) + \mathrm{O_2^g} \rightarrow (\mathrm{O}_i^{if} + \mathrm{V_CO_2}) + \mathrm{CO}^g, \quad (4)$$

and in the latter

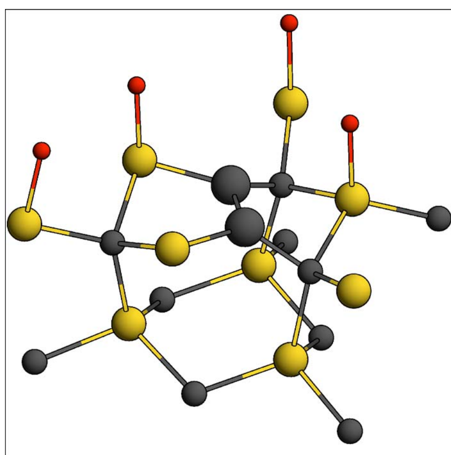

FIG. 4. (Color online) $(C_i)_2$ carbon diinterstitial at the interface, viewed nearly parallel to the SiC surface, SiO_2 on top. [O, small, dark grey spheres (red); C, medium sized black spheres; Si, large, light grey spheres (yellow); defect atoms are marked by large spheres.] The oxygen neighbors of the upper front silicon atoms have been removed from the picture for clarity.

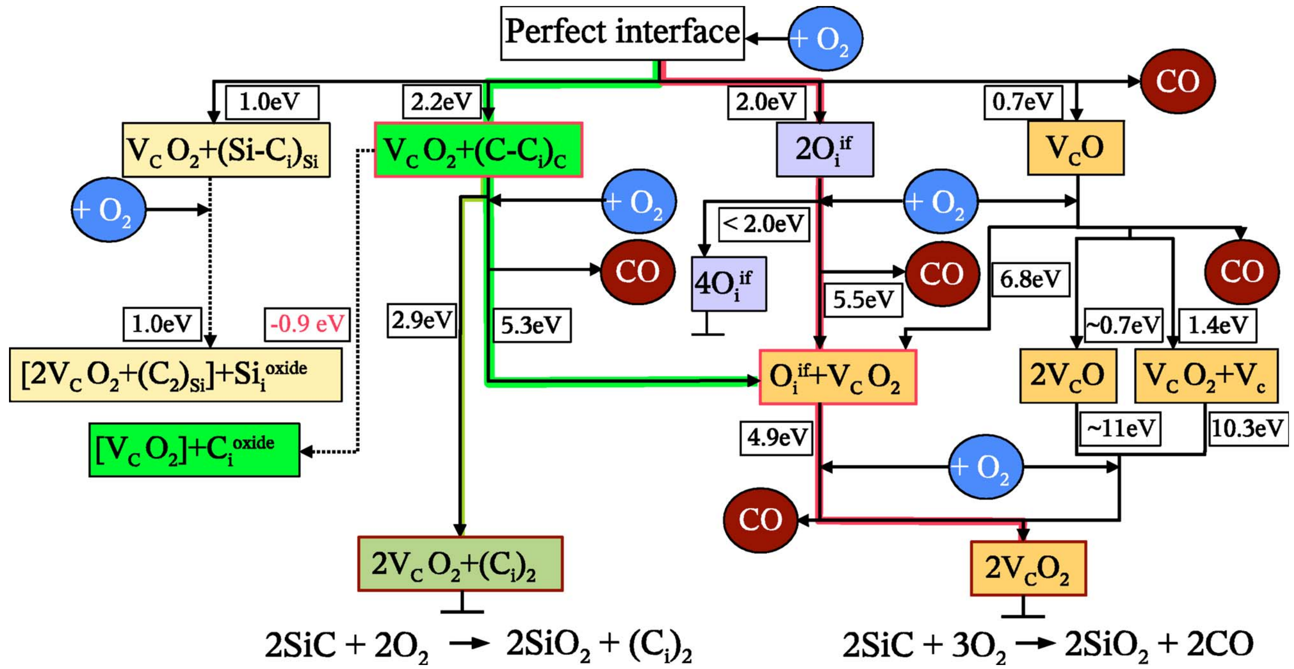

FIG. 5. (Color online) The SiC dry oxidation reaction scheme. Positive energies indicate exother- mic reactions between initial defects of the interface (rectangular frames) and incoming O_2 molecules (round frames) at the beginning of the arrows. The resulting defects (and possible CO molecules) are at the end of the arrow(s) near which the reaction energy is shown. [Equations (2)–(8) were extracted this way from the figure.] The dominant reaction paths are marked by thick lines (green and red).

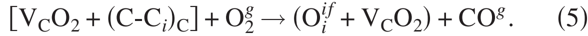

$$[\mathrm{V_CO_2} + (\mathrm{C\text{-}C}_i)_\mathrm{C}] + \mathrm{O}_2^g \rightarrow (\mathrm{O}_i^{if} + \mathrm{V_CO_2}) + \mathrm{CO}^g. \qquad (5)$$

Both these reactions are exothermic, yielding 5.3 eV and 5.5 eV, respectively.

A third O_2 molecule can then remove a second carbon atom by emitting a CO molecule to form a second V_CO_2 unit, thus finishing a stochiometrically complete oxidation cycle,

$$(\mathrm{O}_i^{if} + \mathrm{V_CO_2}) + \mathrm{O}_2^g \rightarrow 2(\mathrm{V_CO_2}) + \mathrm{CO}^g \qquad (6)$$

with an energy gain of 4.9 eV.

The three-step process of oxidation

$$2\ \mathrm{SiC} + 3(\mathrm{O}_2^g) \rightarrow 2\ \mathrm{SiO_2} + 2\ \mathrm{CO}^g \qquad (7)$$

yields a total of 12.4 eV.

The two branches of oxidation described above lead to a chemically perfect oxide and, based on their energetic dominance, can be regarded as the "normal" route of oxidation (with topological rearrangement following). It must be kept in mind, however, that in the course of this process O_i^{if} defects (Si-O-C bridges) and $[V_CO_2+(C\text{-}C_i)_C]$ defects are created temporarily but continuously. When stopping the oxidation process at any time, O_i^{if} and $[V_CO_2+(C\text{-}C_i)_C]$ will remain at the interface in significant concentrations. This explains the observed carbon excess at the interface[3,17] as well as the observed presence of Si-O-C bridges.[11,12] In fact, the end results of these reaction routes (prior to topological rearrangement), the *A*-center-like V_CO_2 defects, are in line with the PAS observations.[18]

Looking at Fig. 5 and starting with the reaction leading to $V_CO_2+(C\text{-}C_i)_C$, a route for permanent carbon incorporation could be considered. As shown in the figure, the reaction

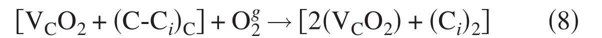

$$[\mathrm{V_CO_2} + (\mathrm{C\text{-}C}_i)_\mathrm{C}] + \mathrm{O}_2^g \rightarrow [2(\mathrm{V_CO_2}) + (\mathrm{C}_i)_2] \qquad (8)$$

leads to an energy gain of 2.9 eV. The result is the very stable and chemically inert dimer, described in the preceding section. Although the energy gain is significant, comparing it to the energy of the alternative reaction (5.3 eV) indicates that the equilibrium concentration ratio between $2(V_CO_2)+(C_2)_i$ and $O_i^{if}+V_CO_2$ would be rather small even at the temperatures of oxidation. However, it must be taken into account, that interstitial carbon is mobile at 1200 °C, as shown in Ref. 51. Since the disproportionation reactions

$$2[\mathrm{V_CO_2} + (\mathrm{C\text{-}C}_i)_\mathrm{C}] \rightarrow [\mathrm{V_CO_2} + (\mathrm{C}_i)_2] + (\mathrm{V_CO_2}), \qquad (9)$$

$$2[\mathrm{V_CO_2} + (\mathrm{C\text{-}C}_i)_\mathrm{C}] \rightarrow [(\mathrm{C}_i)_2] + 2(\mathrm{V_CO_2}) \qquad (10)$$

are exothermic by 0.3 eV and 1.0 eV, respectively, it may be expected after all, that $[V_CO_2+(C_i)_2]$ and $(C_i)_2$ defects will occur in significant quantities. Therefore, alternative to the normal route of oxidation [where $(C\text{-}C_i)$ defects are only temporarily created], carbon incorporation by the formation of $(C_i)_2$ dimers can be expected.

It should also be investigated, whether upon arrival of an O_2 molecule, the emission of C_i into the oxide (i.e., V_CO_2 in the carbide phase and C_i in the oxide phase) is preferred over $V_CO_2+(C\text{-}C_i)_C$ on the carbide side. As is shown on the left-hand side of Fig. 5 such a reaction is endothermic by 0.9 eV. (Note the sign change with respect to Ref. 28, where it was incorrect.) It must be pointed out, however, that our calcula-

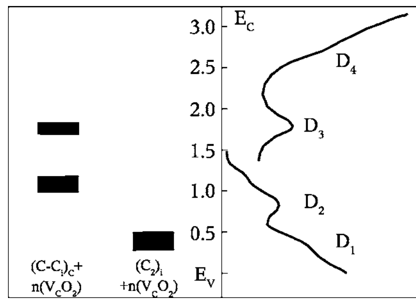

FIG. 6. Environment dependent range of energy levels of the elementary C-C units compared to the observed D_{it} (cf. Introduction) of 4*H*-SiC.

tions on the emission of atoms into the oxide have somewhat higher uncertainty than the interface reaction energies.

Similarly, the results for the emission of a silicon interstitial into the oxide (far left in Fig. 5) has a higher uncertainty. The emitted carbon interstitial could form a split interstitial on a silicon site. The calculated reaction energy, 1.0 eV, is an underestimation because of the large relaxation we find in the oxide phase (which is relatively thin in the model). The next oxidation step, producing a carbon pair on the Si site in the carbide and a Si interstitial in the oxide, also releases a relatively small amount of energy. However, in addition to the solely energetic arguments presented above, one must also consider the specific volumes of Si in SiC and SiO_2, which is larger in SiO_2 by a factor of ~2. Therefore, during the structural rearrangements leading to the vitreous structure of the SiO_2 parts (as mentioned in Sec. III), Si interstitials must be emitted from the interface into the oxide layer, similar to the oxidation process of Si.[52]

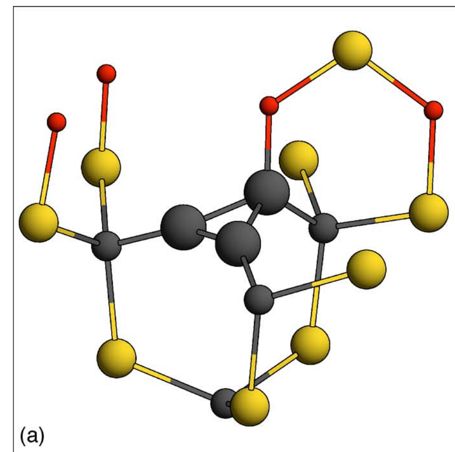

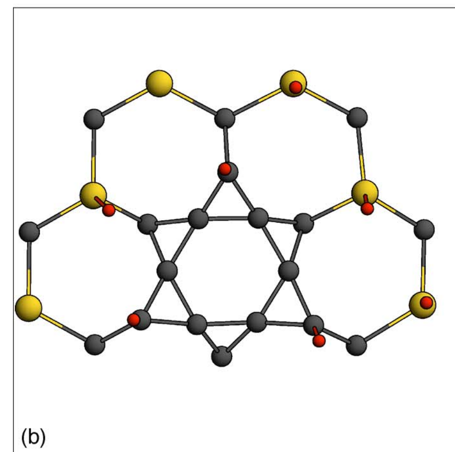

FIG. 7. (Color online) $(C_3)_{Si}$ carbon aggregates at the interface, (a) obe unit viewed nearly parallel to the SiC surface, (b) top view of the interface layer with three neighboring units. [O, small, dark grey spheres (red) C, medium sized black spheres; Si, large, light grey spheres (yellow) defect atoms are marked by large spheres.]

V. CORRELATIONS BETWEEN INTERFACE DEFECTS AND THE D_{it}

Based on the picture emerging from our investigations regarding the reaction routes, we can examine the electronic structure of the interface. As explained above, the oxidation proceeds by producing temporarily O_i^{if}, $V_CO_2+(C-C_i)_C$, and V_CO_2 defects as well as $(C_i)_2$ pairs with varying environments. Only the carbon defects are electrically active.

Let us recall that the $(C\text{-}C_i)_C$ defect has two sp^2-hybridized C atoms sharing a carbon site, with a single bond between them and a pair of nearly orthogonal p orbitals at $E_V+1.4$ eV and at $E_V+1.9$ eV. When this defect is in the direct vicinity of a V_CO_2 unit, these p states are shifted to $E_V+1.0$ eV and $E_V+1.8$ eV, respectively. Depending on the number n of V_CO_2 defects in the neighborhood, the interstitial carbon dimers $(C_i)_2$ at the interface show a doubly occupied state between 0.37 eV and 0.51 eV and no unoccupied state in the gap.[59]

Comparison of these features with the experimentally observed D_{it} of Fig. 1 is shown in Fig. 6. The environment dependent energies of the p states of the singly bonded $(C\text{-}C_i)_C$ and the π bonds of the doubly bonded $(C_i)_2$ defects roughly coincide with the measured structures in the D_{it}. Considering the experimental evidence about carbon excess at the surface, its most likely form is short π-bonded chains or possibly a few aromatic rings (cf. the discussion about the SER results in the Introduction). The donorlike π states introduced by the $(C_i)_2$ defect are characteristic to such type of carbon clusters and their calculated position explains the interface state density near the valence band. [In fact, the calculated range of individual $(C_i)_2$ states seems to fit the structure D_1 quite well.] The pair of p-states of the singly bonded $(C\text{-}C_i)_i$ defects lie closer to midgap, and may well be the origin of the Structures D_2 and D_3, predicting amphoteric behavior for them. By any means, $(C\text{-}C_i)_C$ is the defect, the concentration of which might be modified by reoxidation. In contrast, the very stable $(C_i)_2$ dimers will possibly grow into the oxide. From our results it appears that neither of the possible bonds between sp^2 carbon will cause acceptor states in the upper half of the band gap of 4*H*-SiC. This finding lends support to the assignment of the states in this range to defects in the oxide, instead of carbon defects at the interface. This should be true not only for the "original" NITs, as proposed in Refs. 5, 9, 10, and 27, but also for the second set of NITs,[7] coinciding with the structure D_4 in the observed D_{it}.

Despite all our efforts, we were not able to construct larger, stable, electrically active clusters of carbon interstitials. This may be a shortcoming of the too small simulation cell, but it should be noted, that the $(C_i)_2$ dimers are extremely stable and chemically inert, because of their double bond. Aggregation of such dimers is, however, possible.[53] The inevitable topological rearrangement from V_CO_2 defects of the interface to the vitreous structure of the newly formed silica parts, accompanied by Si emission may lead to the formation of small graphitic structures. In our model, larger clusters of carbon could only be formed at carbon antisites (C_{Si}) which should be abundant, even in as-grown SiC. Figure 7 shows two such clusters, based on the bulk $(C_3)_{Si}$ defect proposed in Ref. 54. The occupied levels corresponding to the C=C double bonds are shifted towards [in the case of Fig. 7(a)] and into [in the case of Fig. 7(b)] the valence band. No acceptor levels appear below the conduction band. Although, the planar hexagon of C atoms in the structure shown in Fig. 7(b) could be a seed for the formation of graphite platelets, our calculations in the present, limited-size model cannot confirm the presence of graphitic bands as an explanation for the background increasing continuously toward the band edges in the D_{it}. Still, the defects shown in Fig. 7 can contribute to the high interface state density near the VB.

VI. CONCLUSIONS

We have investigated the possible defects of the SiC/SiO_2 interface by means of density functional calculations. Using the calculated total energy of stable defect configurations (with respect to incoming O_2 and out-diffusing CO molecules), and assuming thermal quasiequilibrium during oxidation, we could establish energetically favorable reaction routes, leading to a complete oxidation cycle in three steps. Along this route, electrically inactive Si-O-C bridges and *A*-center-like carbon vacancy-oxygen defects, as well as active interstitial carbon atoms are created—temporarily but continuously. Stopping the oxidation at any time, a high concentration of such defects will remain at the interface. The former two defects have, indeed, been observed by XPS and PAS. The interstitial sp^2 carbon atoms form split pairs with lattice C atoms at the interface (forming a single C-C bond), and give rise to a pair of amphoteric deep states in the range of distinct features in the observed D_{it} spectrum. Carbon can be incorporated at the interface in form of doubly bonded interstitial dimers, which cause a band of donor states near the valence band. The predicted range of the levels of such individual defects coincides with a shoulder in the observed D_{it}. Larger carbon clusters (including antisites) investigated in this work, introduce only occupied states near the VB edge. No carbon related unoccupied states have been found near the CB edge.

Our results imply that, beside CO molecules, also carbon interstitials and stable carbon pairs can grow into the oxide, with a concentration decreasing away from the interface. These defects, in addition to Si interstitials (necessarily emitted into the near-interface region due to topological reasons), may be sources of near interface traps. Calculations regarding defects in the oxide will be published separately.

Considering our results, the well known beneficial effect of nitrogen on the interface states might be explained by the differences in the oxidation reactions in the case of oxidation in presence of nitrogen, or by additional reactions between nitrogen and the defects found here, in case of post-oxidation nitrogen annealing. Work in this direction is in progress.

ACKNOWLEDGMENTS

Support by the Hungarian OTKA Grant No. F-038357, and Grant No. PHY010001P from the Pittsburgh Supercomputer Center with Grant No. PHY020013N from the National Center for Supercomputing Applications are appreciated. The authors thank R. P. Devaty for his useful comments on the paper. The authors are grateful for the support and for cooperation from the bilateral DFG contract No.436 UNG113/137/0 (MTA -No. 118).

*Electronic address: Jan.Knaup@phys.uni-paderborn.de
[†]Also at Department of Atomic Physics, Budapest University of Technology & Economics, Budafoki út 8, H-1111, Budapest, Hungary.

[1] V. V. Afanas'ev, M. Bassler, G. Pensl, and M. Schulz, Phys. Status Solidi A **162**, 321 (1997).
[2] G. Y. Chung, C. C. Tin, J. R. Williams, K. McDonald, M. D. Ventra, S. T. Pantelides, L. C. Feldman, and R. A. Weller, Appl. Phys. Lett. **76**, 1713 (2000).
[3] H. Kobayashi, T. Sakurai, and M. Takahashi, and Y. Nishioka, Phys. Rev. B **67**, 115305 (2003).
[4] M. Bassler, G. Pensl, and V. Afanas'ev, Diamond Relat. Mater. **6**, 1472 (1997).
[5] V. V. Afanas'ev, A. Stesmans, M. Bassler, G. Pensl, and M. J. Schulz, Appl. Phys. Lett. **76**, 336 (2000).
[6] N. S. Saks, S. S. Mani, and A. K. Agarwal, Appl. Phys. Lett. **76**, 2250 (2000).
[7] H. Ö. Ólafsson, Ph.D. thesis, Chalmers University of Technology, Microwave Electronics Laboratory, SE-412 96 Göteborg, Sweden, 2004 (unpublished).
[8] T. E. Rudenko, H. Ö. Ólafsson, E. Ö. Sveinbjörnsson, I. P. Osiyuk, and I. P. Tyagulski, Microelectron. Eng. **72**, 213 (2004).
[9] V. Afanas'ev, F. Ciobanu, G. Pensl, and A. Stesmans, *Silicon Carbide - Recent Major Advances* (Springer, New York, 2003).
[10] V. Afanas'ev, F. Ciobanu, S. Dimitrijev, G. Pensl, and A. Stesmans, J. Phys.: Condens. Matter **16**, 1839 (2004).
[11] B. Hornetz, H.-J. Michel, and J. Halbritter, J. Mater. Res. **9**, 3088 (1994).
[12] G. G. Jernigan, R. E. Stahlbush, and N. S. Saks, Appl. Phys. Lett. **77**, 1437 (2000).
[13] C. Virojanadara and L. Johansson, Surf. Sci. Lett. **472**, L145 (2001).

[14] V. R. Vathulya, D. N. Wang, and M. H. White, Appl. Phys. Lett. **73**, 2161 (1998).
[15] S. Wang, M. Di Ventra, S. G. Kim, and S. T. Pantelides, Phys. Rev. Lett. **86**, 5946 (2001).
[16] V. V. Afanas'ev, A. Stesmans, and C. I. Harris, Mater. Sci. Forum **264–268**, 857 (1998).
[17] K. Chang, N. Nuhfer, L. Porter, and Q. Wahab, Appl. Phys. Lett. **77**, 2186 (2000).
[18] J. Dekker, K. Saarinen, H. Olafsson, and E. O. Sveinbjornsson, Appl. Phys. Lett. **82**, 2020 (2003).
[19] W. Lu, L. Feldman, Y. Song, S. Dhar, W. Collins, W. Mitchel, and J. R. Williams, Appl. Phys. Lett. **85**, 3495 (2004).
[20] C. Castiglioni, C. Mapelli, F. Negri, and G. Zerbi, J. Chem. Phys. **114**, 963 (2001).
[21] J. L. Cantin, H. J. von Bardeleben, Y. Shishkin, Y. Ke, R. P. Devaty, and W. J. Choyke, Phys. Rev. Lett. **92**, 015502 (2004).
[22] M. Johnson, M. Zvanut, and O. Richardson, J. Electron. Mater. **29**, 368 (2000).
[23] M. Di Ventra and S. T. Pantelides, Phys. Rev. Lett. **83**, 1624 (1999).
[24] H. Li, S. Dimitrijev, H. Harrison, and D. Sweatman, Appl. Phys. Lett. **70**, 2028 (1997).
[25] P. Lai, S. Chakraborty, C. Chan, and Y. Cheng, Appl. Phys. Lett. **76**, 3744 (2000).
[26] P. Jamet and S. Dimitriev, Appl. Phys. Lett. **79**, 323 (2001).
[27] V. V. Afanas'ev, A. Stesmans, F. Ciobanu, G. Pensl, K. Y. Cheong, and S. Dimitrijev, Appl. Phys. Lett. **82**, 568 (2003).
[28] P. Deák, A. Gali, J. Knaup, Z. Hanjal, T. Frauenheim, P. Ordejón, and W. J. Choyke, Physica B **340–342**, 1069 (2003).
[29] A. Bongiorno and A. Pasquarello, Phys. Rev. B **70**, 195312 (2004).
[30] C. Köhler, Z. Hajnal, P. Deák, T. Frauenheim, and S. Suhai, Phys. Rev. B **64**, 085333 (2001).
[31] C. Radtke, I. Baumvol, B. Ferrera, and F. Stedile, Appl. Phys. Lett. **85**, 3402 (2004).
[32] H. J. Monkhorst and J. D. Pack, Phys. Rev. B **13**, 5188 (1976).
[33] T. Frauenheim, G. Seifert, M. Elstner, Z. Hajnal, G. Jungnickel, D. Porezag, S. Suhai, and R. Scholz, Phys. Status Solidi B **217**, 41 (2000).
[34] J. M. Soler, E. Artacho, J. D. Gale, A. García, J. Junquera, P. Ordejón, and D. Sánchez-Portal, J. Phys.: Condens. Matter **14**, 2745 (2002).
[35] N. Troullier and J. L. Martins, Phys. Rev. B **43**, 1993 (1991).
[36] D. M. Ceperley and B. J. Alder, Phys. Rev. Lett. **45**, 566 (1980).
[37] J. P. Perdew and A. Zunger, Phys. Rev. B **23**, 5048 (1981).
[38] A. Gali, P. Deák, P. Ordejón, N. T. Son, E. Janzén, and W. J. Choyke, Phys. Rev. B **68**, 125201 (2003).
[39] P. Deák, A. Gali, A. Sólyom, P. Ordejón, K. Kamarás, and G. Battsig, J. Phys.: Condens. Matter **15**, 4767 (2003).
[40] A. D. Becke, J. Chem. Phys. **98**, 5648 (1993).
[41] J. Perdew, M. Ernzerhof, and K. Burke, J. Chem. Phys. **105**, 9982 (1996).
[42] J. Muscat, A. Wander, and N. Harrison, Chem. Phys. Lett. **34**, 397 (2001).
[43] J. Heyd and G. Scuseria, J. Chem. Phys. **121**, 1187 (2004).
[44] A. Becke, J. Chem. Phys. **104**, 1040 (1996).
[45] V. R. Saunders *et al.*, *CRYSTAL2003 Users's Manual* (University of Torino, Torino, 2003).
[46] J. C. Barthelat and P. Durand, Mol. Phys. **33**, 159 (1977).
[47] M. Causá, R. Dovesi, and C. Roetti, Phys. Rev. B **43**, 11937 (1991).
[48] A. Gali, D. Heringer, P. Deák, Z. Hajnal, T. Frauenheim, R. P. Devaty, and W. J. Choyke, Phys. Rev. B **66**, 125208 (2002).
[49] G. D. Watkins and J. W. Corbett, Phys. Rev. **121**, 1001 (1961).
[50] J. W. Corbett, G. D. Watkins, and R. S. McDonald, Phys. Rev. **135**, A1381 (1964).
[51] M. Bockstedte, A. Mattausch, and O. Pankratov, Phys. Rev. B **69**, 235202 (2004).
[52] C. Scofield and A. Stoneham, Semicond. Sci. Technol. **1**, 215 (1995).
[53] M. Bockstedte (private communication).
[54] A. Mattausch, M. Bockstedte, and O. Pankratov, Phys. Rev. B **69**, 045322 (2004).
[55] P. Deák, A. Gali, A. Sólyom, A. Buruzs, and T. Frauenheim, J. Phys.: Condens. Matter (to be published).
[56] It should be noted that the valence band (VB) offset between SiC polytypes is small, and the level positions of similar defects with respect to the VB edge is also similar in 6*H*-SiC and 4*H*-SiC.
[57] Tests in bulk Si have shown (Ref. 55) that the accuracy of all calculated properties can be consistently increased by optimizing the mixing ratio. Since we use the hybrid functional calculations on analogous bulk defects only for correction purposes, the loss of transferability is an acceptable trade-off.
[58] The defect geometries were found in quasistaic minimization of the energy, not by molecular dynamics.
[59] The size of the model does not allow a constant accuracy with increasing n in the level positions of such large defects, due to the increasingly limited relaxation freedom. Therefore, we just quote the energy range in which we find the states.